Single-molecule vibrational pumping in SERS

C. M. Galloway, E. C. Le Ru* and P. G. Etchegoin*

Single-molecule vibrational pumping in surface-enhanced Raman scattering (SERS) is demonstrated rigorously using the bi-analyte SERS method at low temperatures. These experiments reveal a systematic difference between the radiative SERS cross section estimated from the Stokes intensity and that obtained by pumping itself (from the anti-Stokes-to-Stokes ratio), the latter being always larger. This difference can only be reliably demonstrated in the single-molecule SERS regime, for it is otherwise affected by complications of the averaging (over the enhancement distribution) of the signals of several molecules. The findings in this paper highlight the limitations of the pumping cross-section, which cannot (in general) be taken as a reliable measure of the SERS cross-section itself. We provide a discussion of the main possible explanations for the systematic difference of the two estimates.

I. Introduction

The surface-enhanced Raman scattering (SERS) cross section is, arguably, the most important characteristic of the effect. After all, a huge amount of research effort has been invested on SERS over the years simply because it *amplifies* the (otherwise small) normal Raman cross section.[1,2] The amplification, in fact, can go all the way to make single-molecule observation a routine.[3] Understanding all the details that are directly or indirectly related to the SERS cross section, as well as properly quantifying its values in different situations, is no doubt fundamental for a better understanding of the effect. Surprisingly though, ~ 30 years after the first reports of the effect[4–6] there are still several very basic aspects of the SERS cross section that have not yet been explored, or even measured, and it is only relatively recently that reliable values for SERS cross sections of crucial cases (like single-molecule SERS cross sections) have been reported.[7] Implicit in the determination of SERS cross sections is the value of the *enhancement factor*, which can be obtained from the former if a reliable value for the bare (non-SERS) cross section is known. With exceptions to the rule (notably, the case of Crystal Violet treated later[7]) the latter cannot be obtained for resonant excitation of dyes, because of the overwhelming dominance of fluorescence. But it is known in many other cases for important SERS probes under pre-resonance or non-resonance conditions,[7] and for some resonant probes using special techniques.[8] The accurate determination of the SERS cross sections for the latter has provided reliable figures for the SERS enhancement factor and has allowed a direct comparison with theoretical estimates.[3]

This paper is about one of the aspects of the SERS cross section that have not been hitherto widely considered: the exact meaning of the vibrational pumping cross section. Its importance relies not only in the understanding of a subtle aspect of the SERS process, but also in the reconciliation of the experimental estimates of SERS cross sections obtained from vibrational pumping;[7,9–12] the latter have been (historically) larger than estimates obtained by other more conventional methods.[7,12] For more than one reason then, finding clear evidence for the exact meaning of the pumping cross sections represents, in our view, an important yardstick in our understanding of the microscopic origin of the effect. The demonstration of vibrational pumping in single molecules under SERS conditions provides a way of ruling out certain potential problems, like the possible effect of the averaging of the signals. In that way it provides a much clearer meaning to the pumping cross sections in SERS and highlights both its potential and limitations.

II. A simple model of SERS vibrational pumping

A The pumping cross-section

A full description of the mathematical modeling underpinning the phenomena of vibrational pumping (in terms of a rate equation for the vibrational population) has been given already in ref. 12. However, for the sake of clarity and consistency, we shall repeat a few key steps here. This is important, in particular, to emphasize those places where the introduction of the distinction between *ensemble averages* of signals or *single-molecule* conditions is introduced; a situation that has not been explicitly considered in the past.[9–12] In addition, we distinguish from the beginning the pumping cross section as a separate identity, rather than forcibly associating it with the Stokes cross section (which can be measured independently in the single-molecule regime). In this manner, we can claim to measure both cross section independently and a direct comparison between the two can be, thereafter, established. Whether the Stokes cross section is fully responsible or not for the vibrational population observed on the anti-Stokes side is something that will be decided by the experiment, rather than being imposed in the analysis from the start.[9–12]

The MacDiarmid Institute for Advanced Materials and Nanotechnology, School of Chemical and Physical Sciences, Victoria University of Wellington, PO Box 600, Wellington, New Zealand. E-mail: Eric.LeRu@vuw.ac.nz, Pablo.Etchegoin@vuw.ac.nz

Let us consider a single vibrational mode for one molecule that is in a steady state. The rate of change of the vibrational population (n) is zero and given by (when $n \ll 1$, which is always the case here):[12]

$$\frac{dn}{dt} = \frac{\sigma^{pump} I_L}{\hbar \omega_L} + \frac{\exp(-\hbar \omega_\nu / k_B T)}{\tau} - \frac{n}{\tau} = 0, \quad (1)$$

where the first two terms correspond to an increase in the vibrational population due to pumping and thermal excitation, respectively. I_L and ω_L are the power density [W m^{-2}] and frequency [rad s^{-1}] of the laser. The final term is the decay rate due to the finite lifetime (τ [s]) of the vibration (population relaxation). At low temperatures (which for the vibrations of interest here means $T \sim 80$ K, or lower) the contribution from the thermal excitation rate (second term in eqn (1)) is negligible relative to the pumping rate (first term in eqn (1)). Hence, eqn (1) can be rearranged to give:

$$n = \frac{\sigma^{pump} I_L \tau}{\hbar \omega_L}. \quad (2)$$

As mentioned before, we make here the explicit distinction that the cross section populating the level in the rate equation is a *pumping cross section*. The only pumping mechanism considered so far in previous studies[9–12] is the vibrational population created for each Stokes–Raman process detected in the far-field. If this is indeed the only mechanism operating, then the pumping cross-section should be equal to the total radiative SERS Stokes cross-section, *i.e.* the differential radiative SERS Stokes cross-section integrated over all possible detection directions (over solid angles $\delta\Omega$).[2] The total cross section σ_S^{rad} can in fact be approximately derived from the (more directly measurable) differential one by means of:[2,13]

$$\sigma_S^{rad} = \frac{8\pi}{3} \frac{1 + 2\rho_{dep}}{1 + \rho_{dep}} \left(\frac{d\sigma_S^{rad}}{d\Omega}\right)_{SM} \sim 10 \left(\frac{d\sigma}{d\Omega}\right)_{SM}, \quad (3)$$

where ρ_{dep} is the *depolarization ratio* of the mode, whose effect can be ignored in a first approximation. One of the goals of this study is to check the assumption made so far that $\sigma^{pump} \approx \sigma_S^{rad}$, and we therefore allow for them to be different in our analysis. We will in fact demonstrate that (in general) the pumping cross section will *not* be the same as the total radiative Stokes SERS cross-section.

B Ensemble averaging of the pumping equations

Most SERS vibrational pumping studies so far were carried out in the many-molecule regime (or any claim of single-molecule regime were not rigorously justified). The solutions of the pumping rate equations must in this case be ensemble-averaged.

Using eqn (2) for the vibrational population n, the anti-Stokes and Stokes intensities [W] for an *ensemble* of N molecules (again assuming $n \ll 1$; *i.e.* no stimulated scattering) are given by:[11,12]

$$I_S = N \langle d\sigma_S^{rad}/d\Omega \rangle I_L, \quad (4)$$

and

$$I_{aS} = \frac{N \langle \sigma^{pump} d\sigma_{aS}^{rad}/d\Omega \rangle \tau I_L^2}{\hbar \omega_L}, \quad (5)$$

where $d\sigma_S^{rad}/d\Omega$ and $d\sigma_{aS}^{rad}/d\Omega$ are the differential SERS Stokes and anti-Stokes radiative cross sections. The brackets $\langle \cdots \rangle$ in eqn (4) and (5) represent the *spatial averaging* over all of the molecules N (which might be subject to widely varying enhancement factors at different positions[3,14]). Note, one more time, the explicit distinctions between *radiative* and *pumping* cross sections in eqn (4) and (5). The Stokes signal is purely radiative; it is proportional to $d\sigma_S^{rad}/d\Omega$ and does not depend on the population n. The anti-Stokes signal, on the other hand, is proportional to the differential radiative cross section at the anti-Stokes frequency (in general $d\sigma_{aS}^{rad}/d\Omega \neq d\sigma_S^{rad}/d\Omega$), but it is also proportional to the population n, which is $\propto \sigma^{pump}$. We obtain, then, a mixture of dependencies on radiative and pumping cross sections in the equations. We do not force σ^{pump} to be identical to the total radiative SERS cross-section, σ_S^{rad}, but rather expect the experiment to tell us if this is actually the case, thus revealing its microscopic origin.

From eqn (4) and (5) we get for the anti-Stokes-to-Stokes ratio (ρ) at low temperatures:

$$\rho = \frac{I_{aS}}{I_S} = \frac{\langle \sigma^{pump} d\sigma_{aS}^{rad}/d\Omega \rangle}{\langle d\sigma_S^{rad}/d\Omega \rangle} \frac{\tau I_L}{\hbar \omega_L}. \quad (6)$$

By introducing the *asymmetry factor* $A = \sigma_{aS}^{rad}/\sigma_S^{rad}$,[10–12] eqn (6) can be written as:

$$\rho = \frac{\langle A \sigma^{pump} d\sigma_S^{rad}/d\Omega \rangle}{\langle d\sigma_S^{rad}/d\Omega \rangle} \frac{\tau I_L}{\hbar \omega_L}. \quad (7)$$

The effect of the spatial averaging process $\langle \cdots \rangle$ in eqn (7) is not trivial, and has been partially studied in ref. 11. Obviously, the $d\sigma_S^{rad}/d\Omega$ in the numerator cannot be directly simplified with the one in the denominator, for they are both affected differently by the averaging process. The fact that SERS enhancement factors at hot-spots normally follow a *long-tail distribution*[2,3,14] places a heavy weight on the highest enhancement factors available in the system, due to the $\sim \sigma^2$ proportionality in the numerator of eqn (7) (if we ignore temporarily the distinction between Stokes and pumping cross sections). This argument has been used to justify the (normally higher) estimates of cross sections that come out from vibrational pumping,[11] and there is also the fleeting question of how feasible it is to take the asymmetry parameter (A) outside the averaging process. This puts then several natural restrictions to the conclusions one can obtain from experiments where a large number of molecules are involved in the signals.

C Single-molecule SERS vibrational pumping

The situation is greatly simplified in the *single-molecule SERS* (*SM-SERS*) *regime*, in which no averaging process is required. In that case, the anti-Stokes-to-Stokes ratio simply reads:

$$\rho = \frac{A \sigma^{pump} \tau I_L}{\hbar \omega_L}. \quad (8)$$

Hence, it is obvious from eqn (8) that the cross-section estimated in vibrational pumping of a single molecule through ρ is the *pumping cross-section*. It is also important to recognize that this expression is actually independent of photobleaching problems, since both the anti-Stokes and Stokes signal increases linearly with time and, as a result, the ratio will be

This journal is © the Owner Societies 2009

Phys. Chem. Chem. Phys., 2009, **11**, 7372–7380 | 7373

independent of the lifetime of the molecule. The advantage of performing the experiments in the single-molecule regime is twofold: (i) it allows a direct estimation of the pumping cross section without any complications from the averaging process, and (ii) it provides, by the same token, an estimate of the *differential radiative cross section* (and therefore the total radiative cross-section using eqn (3)) by direct comparison of the SERS Stokes intensity with a reference compound (of known cross section). This is how enhancement factors of single molecules have been determined in the past,[7] and it then acts as a consistency check by providing direct evidence for the link between σ^{pump} and $d\sigma_S^{rad}/d\Omega$.

The values of the pumping and radiative cross sections are, obviously, strongly dependent on the specific molecule under observation. Both are intimately related to the problem of the *SERS enhancement factor for single molecules* and this is known (and expected) to be strongly dependent, for example, on the exact microscopic location of the molecule. Differences of a fraction of a nanometer (comparable to typical molecular sizes) are known to produce substantial differences[2,3] for the enhancement factor and SERS cross sections of single molecules. A robust conclusion on the comparison between the pumping and radiative Stokes cross section, accordingly, cannot be inferred from measurements on a single case; but rather copious statistics of single-molecule SERS pumping events are required to sample many characteristic cases. Our aim here is, therefore, to measure large statistics of pumping and Stokes (radiative) cross-sections simultaneously for a large set of single-molecule SERS pumping events at low temperatures. As for standard (non-pumping) SM-SERS experiments, the single-molecule nature of the signal cannot be inferred simply from concentration estimates.[3,15] As a much more rigorous approach to this problem, we therefore apply here the bi-analyte SERS technique.[15,16]

III. Experimental methods

Experiments have been carried out under standard conditions that were reported elsewhere.[15–17] We will then keep the details to a minimum, avoiding as much repetition as possible. We do, however, provide all the relevant parameters necessary for a quantification of the cross-sections by the different approaches, which is the main point of this paper.

The samples were prepared by mixing 0.5 mL of citrate-reduced Ag colloids (Lee & Meisel[18]) with 0.5 mL of 20 mM KCl and a premixed solution of Nile Blue (NB) and Crystal Violet (CV), such that the final concentration for each dye was 1 nM. These dyes are going to be used here as bi-analyte SERS partners to isolate single-molecule events.[15–17]

Nevertheless, unlike conventional bi-analyte SERS situations, these experiments are performed under the conditions needed for vibrational pumping (*i.e.*, low temperatures and observing the Stokes and anti-Stokes sides of the spectra simultaneously). In addition, these dyes were chosen for they have resonances (at ~ 628 nm and ~ 590 nm, respectively) that are close to the wavelength of the HeNe-laser (633 nm) used here as excitation. The colloids and their SERS performance for single molecule SERS have been studied in full detail elsewhere.[15,20] The final solution is drop-casted after a few minutes (allowing for adsorption of the dye onto the colloids) onto a silicon wafer which has been previously coated with a thin layer of poly-L-lysine, as described in ref. 15. After leaving the solution drying on the substrate under a mild heat for ~ 30 min, the rest is siphoned off with a glass pipette and allowed to dry completely thereafter. This forms a sample that consists of a relatively low density of isolated colloidal aggregates (strongly grafted to the substrate through the poly-L-lysine layer), such that there are only a few hot-spots created (within the area of the laser spot; ~ 1.5 μm in diameter for the $\times 50$ long working distance objective, NA = 0.5 in air). Together with the low concentration of dyes, this allows us to identify single molecule events with the bi-analyte method.[15] After the sample has dried, it is placed in a cryostat for microscopy, and stays thereafter in a nitrogen gas atmosphere (so ice crystals do not form on the sample), whilst lying on the cold finger of the cryostat, which is held at 77 K for the entire experiment.

Raman measurements were taken with an incident power of 0.5 mW (at 633 nm) with no polarization analysis. A Jobin Yvon LabRam spectrometer (with a holographic notch filter) attached to a BX2 Olympus microscope was used. Measurements are performed with a 300 lines per mm diffraction grating blazed in the red. The grating we use allows us to simultaneously observe both the Stokes and anti-Stokes signals of several peaks (up to 1300 cm^{-1} on both sides of the laser). We have therefore chosen dyes that are resonant in the red and restricted ourselves to measuring the low energy modes; up to 1300 cm^{-1} only.

A beam and throughput characterization with a reference sample is necessary in order to calibrate the response of the system and deduce the cross-section of a single molecule event from the measured intensity (in counts s^{-1}) with respect to a compound of known differential Raman cross-section.[7] The beam characterization process has been described in full detail in ref. 7. The throughput test is achieved by a comparison to a molecule with a known cross-section; in this case we have chosen to observe nitrogen in air, which has a differential cross-section of 1.6×10^{-31} cm^2 sr^{-1} at 633 nm excitation.[2,13] The total number of nitrogen molecules in the scattering volume of the objective (~ 131 μm^3) is approximately 3×10^9, taking room temperature as 290 K, atmospheric pressure, and a nitrogen content of 78% in air. From the calibration against nitrogen gas (using long integration times of 120 s) we calculated that the N$_2$ Raman mode at ~ 2331 cm^{-1} has an intensity of 1.54×10^{-8} counts s^{-1} per molecule which corresponds to a conversion factor of $K = 1.065 \times 10^{-23}$ cm^2 s counts^{-1} sr^{-1} for other signals measured under the same experimental conditions. The differential cross-section of a single molecule event in the bi-analyte SERS method, therefore, can be calculated from:

$$\left(\frac{d\sigma_S^{rad}}{d\Omega} \right)_{SM} = KI_S, \qquad (9)$$

where I_S is the integrated intensity of the Stokes signal in counts s^{-1}. Eqn (9) will be used to measure the differential cross-section $(d\sigma_S^{rad}/d\Omega)_{SM}$ of a single molecule event (by relating it to the differential cross section of N$_2$ under identical

experimental conditions). The total cross section σ_S^{rad} can then be obtained from the differential one in eqn (9) by means of eqn (3) discussed earlier. On the contrary, the pumping cross-section σ^{pump} will be calculated from the anti-Stokes to Stokes intensity ratio for single molecule events using eqn (8), with an estimation for A and τ (to which we shall return afterwards).

IV. Results and analysis

A Experimental results

Typical SERS spectra for CV and NB are shown in Fig. 1. Careful consideration had to be taken when deciding which peaks to measure. The energy of the mode had to be large enough so that a significant contribution to n would not be created through thermal population[12] (second term in eqn (1)), but due to the limited size of the spectral window of the CCD the mode energy had to be less than ~ 1300 cm^{-1} (in order to observe the Stokes and anti-Stokes sides simultaneously). Furthermore, the SERS cross-section had to be large enough to observe vibrational pumping. We therefore decided to use the 592 cm^{-1} mode of NB, and the 802 cm^{-1}, 914 cm^{-1}, and 1173 cm^{-1} modes of CV. Crystal Violet has more modes than NB that satisfy simultaneously the list of conditions outlined above.

Spatial mappings[15] were done over a total area of approximately 6400 μm^2, with a measurement taken every 2 μm. Fig. 2 shows a single spatial mapping of 1600 spectra taken at 77 K in which the total integrated intensity per event, in counts per second, is plotted as a function of position. Each spectrum
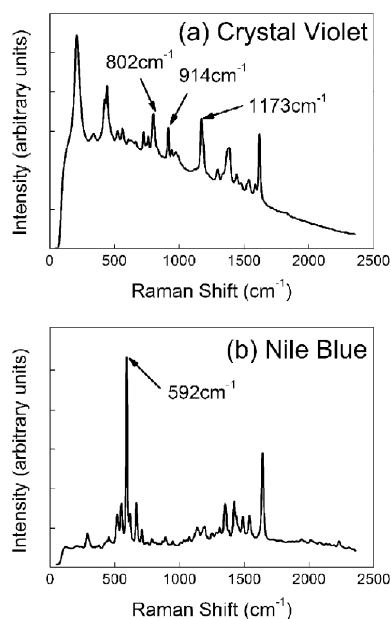

Fig. 1 Typical SERS spectra for (a) Crystal Violet (CV) and (b) Nile Blue (NB). Peaks of interest are the 802 cm^{-1}, 914 cm^{-1} and 1173 cm^{-1} of CV, and the 592 cm^{-1} mode of NB. These peaks were chosen as they have large enough frequencies (ω_v) to be unaffected by heating at 77 K (the Boltzmann term in eqn (1) is negligible for these modes at 77 K) but they are still within the spectral window of the 300 lines mm^{-1} grating to observe the Stokes and anti-Stokes sides simultaneously.
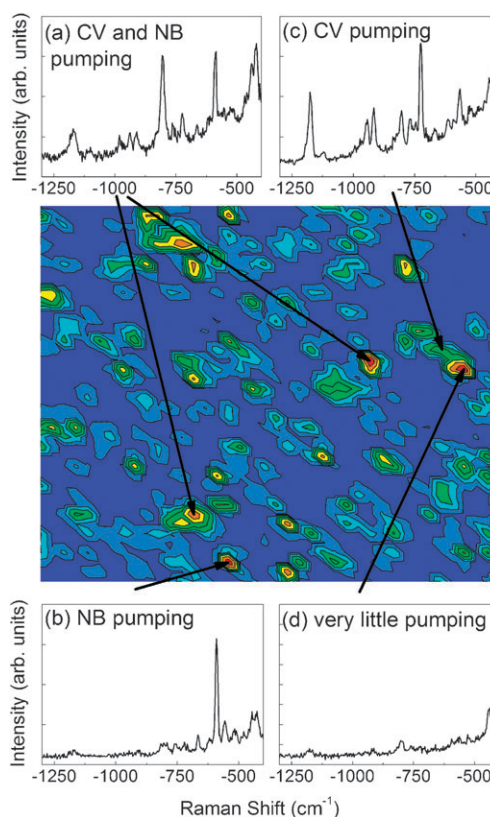

Fig. 2 A contour plot of the total integrated intensity (for both the Stokes and anti-Stokes side), in counts per second, as a function of spatial position for a 2D-mapping. The scale is logarithmic, with blue (red) corresponding to low (high) intensity. Also included are four plots of the anti-Stokes signal for five different positions on the sample, each with a high overall intensity and different levels of pumping; (a) pumping of both NB and CV, (b) pumping of only NB, (c) pumping of only CV (the peak close to -600 cm^{-1} is not the -592 cm^{-1} mode of NB but actually the -563 cm^{-1} mode of CV which has been enhanced strongly by the plasmon resonance), and (d) very little pumping of either dye.

is integrated for 0.2 s which was deemed short enough to minimize any possible effect of photobleaching for our excitation density of 4.48×10^8 W m^{-2}. Measurements (not shown here) were also performed to confirm that the Stokes intensity approximately scaled with excitation density.

From Fig. 2, we can see that the sample contains many regions of high enhancement; a fraction of which are large enough for pumping to be observed. Fig. 2 also contains the anti-Stokes spectrum for five interesting positions on the mapping, all of which have extremely large overall intensities. In Fig. 2(a) we can see two positions in which there is pumping of both dyes simultaneously. It is therefore obvious that we are not observing a single molecule pumping event, but most likely a region with multiple hot-spots (large enough for pumping to be observed), and many (at least two) molecules. Fig. 2(b) and (c) however show two positions in which there is only pumping of one dye or the other, and hence strong candidates for single molecule pumping events. Similar combinations of single-molecule pumping events had already been briefly reported before in ref. 12.
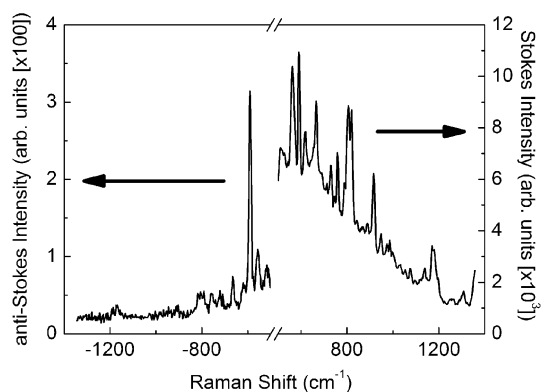
This journal is © the Owner Societies 2009

Phys. Chem. Chem. Phys., 2009, **11**, 7372–7380 | 7375

Fig. 3 The spectrum for a bi-analyte SERS event in which both NB and CV are observed on the Stokes side, but only NB on the anti-Stokes (under pumping conditions at 77 K). The anti-Stokes side provides a much "sharper" contrast of single-molecule conditions because of its $\sim \sigma^2$ proportionality.

A key point to note here is that single molecule pumping does *not* necessarily mean a single molecule event on the Stokes side of the spectrum. This is because the anti-Stokes signal under pumping conditions is much more sensitive to the enhancement than the Stokes one; it is possible to have molecules in weaker hot-spots observed on the Stokes side but not on the anti-Stokes, as shown in Fig. 3. Furthermore, it is also possible to have a region in which many hot spots form, but none that is strong enough to observe pumping on the anti-Stokes side. This is exactly what we see in Fig. 2(d) where the Stokes intensity can be large, but there is very little evidence of pumping on the anti-Stokes side (a many molecules event). Vibrational pumping provides therefore an additional tool to understand in more detail the microscopic origin of the signal.

Qualitatively, we can say that the anti-Stokes signals under vibrational pumping conditions present a different type of "filter" (weighted, approximately, by the square of the cross section ($\sim \sigma^2$) if we ignore temporarily the differences among σ^{pump}, σ_{aS}^{rad}, and σ_S^{rad}). This is clear in eqn (4)–(5) from the fact that the anti-Stokes signal is $\propto \sigma^2$, while the Stokes one is $\propto \sigma$, and the fact that a long-tail distribution of enhancements (typical of hot-spots) produces a much more marked contrast of single molecule situations on the anti-Stokes side in pumping. As a result, there can be different criteria based on the bi-analyte SERS method based on anti-Stokes or Stokes signals to distinguish single molecule cases. The will be an additional contribution to the relative intensities of the anti-Stokes and Stokes signal from the resonance properties of the molecule and the plasmon resonance[19] that will be discussed later.

We found in our data that the anti-Stokes signals provide a much clearer distinction to decide on single-molecule events (in the bi-analyte SERS sense). This is to some degree expected due to the different weights of the enhancement factor distribution for both cases. However, it does mean that (sometimes) a spectrum will be classified as "single-molecule" from the anti-Stokes side, while there might be contributions from more than one molecule on the Stokes one. For example, consider a cluster where we have 5 molecules of NB and 5 of

CV. We ignore for this qualitative argument the difference between pumping and radiative cross sections (making them all of the same order of magnitude). One molecule of NB is subject to a cross section of, say, $\sigma \sim 20$ (in some arbitrary—but same for all—units). The other four NB molecules are subject to a cross section of $\sigma \sim 1$ and the five CV ones are also subject to $\sigma \sim 1$. On the Stokes side, this will constitute a spectrum with a total signal of NB being five times larger than that of CV; *i.e.* 20% percent of the intensity will attributed to the presence of CV and this will not be classified as a single molecule event in the bi-analyte SERS method. In addition, the intensity of the Stokes peak of NB will be made out of one molecule contributing five times more that the other four molecules together (80% of the NB signal is being contributed by a single molecule). On the anti-Stokes side, on the other hand, the spectrum will look very different. Both, the total contribution of the four NB molecules, or the five CV molecules, at $\sigma \sim 1$ will be, by themselves, only $\sim 1\%$ (and probably within the noise level of the spectrum) of the signal contributed by the single NB molecule at $\sigma \sim 20$; *i.e.* the anti-Stokes side will be completely dominated by this one molecule and it will be classified as a single molecule event within the framework of this modified bi-analyte SERS approach based on pumping.

Still, if we now take the ratio of anti-Stokes to Stokes signals of NB as a measure for ρ in eqn (6), this value could be underestimated in general because the Stokes signals may contain contributions from more than one molecule. With this drawback in mind, however, there are very good reasons to use in this problem the anti-Stokes side to decide on single-molecule conditions in the bi-analyte SERS method. Among them, the presence of SERS backgrounds (surface-enhanced fluorescence[21]) which makes the discrimination of single molecule events on the Stokes side more cumbersome than that on the anti-Stokes side. We used the bi-analyte SERS technique on the anti-Stokes side, bearing in mind that its discrimination of single molecule events for the estimation of ρ can result in an underestimation (and therefore in an underestimation of σ^{pump}).

B Measurements of the pumping and stokes cross-sections

We searched for single molecule-pumping events in the 2D-maps by using the modified principal component analysis (MPCA) method developed in ref. 16. This is, however, a matter of convenience and it is not actually crucial. Any analysis method that can isolate the relative proportion of the signal of one dye with respect to the other for a given spectrum can achieve essentially the same result. We use the MPCA method, however, because we have tested it several times in bi-analyte single molecule SERS conditions[16,17,22] and it provides a fast and reliable way to sort out a huge amount of information towards a specific goal. We performed MPCA in the range -550 cm^{-1} to -850 cm^{-1} (anti-Stokes side), which was the obvious choice as it encompasses a mode of both NB and CV with reasonably large cross-sections. It also allows us to identify *only* those events that contain pumping and (with the limitations highlighted in the previous section in place) it provides a fast shortcut towards the events that are really of interest from the vibrational pumping point of view.

Fits were done to the Stokes and anti-Stokes peaks labeled in Fig. 1, by way of a simple intensity integration with a linear fit to the background under the peak, for those spectra that were defined as being single molecule pumping events by the MPCA method.[16] As in ref. 16, we also placed a lower limit on the peak intensities (which depended on the mode) below which the events are discarded due to low signal to noise ratio.

Fig. 4 shows the pumping and total radiative Stokes cross-sections for each of the modes labeled in Fig. 1, for those events that were identified as being single molecule pumping events of a large enough intensity above the noise on the anti-Stokes side. Initially we assume a (realistic) τ of ~ 1 ps[11] and we set $A = 1$ in eqn (8) to obtain σ^{pump}. The possible effects of this not being the case are discussed in detail afterwards (*vide infra*). Both the pumping and radiative Stokes cross-section, and also their ratio, fluctuate by several orders of magnitude for all of the cases due to the different local conditions felt by the molecules. However, that does not prevent the obvious conclusion that there is a marked difference in the average pumping and Stokes cross-section (radiative). The ratio of the pumping and Stokes cross-sections shown in Fig. 4 for most events is typically ~ 10. However, there are many events that have a ratio that is 1 or 2 orders of magnitude larger than the median such that the mean ratio is ~ 100.

Hitherto, the experimental facts stand by themselves: we have established that there is a statistically significant difference between the deduced pumping and Stokes cross sections for single molecule events in SERS (note the logarithmic scale in Fig. 4). Taking into account that ρ might be underestimated as explained earlier, this difference could even be slightly larger than what Fig. 4 suggests. We will now discuss the possible explanations for this spectacular discrepancy.
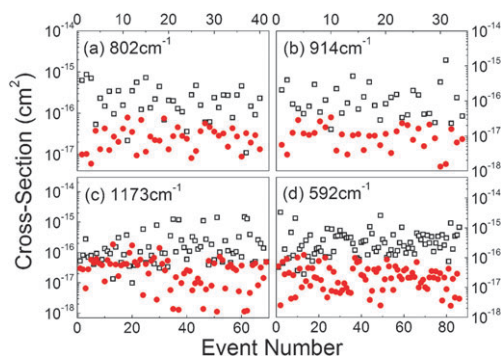

Fig. 4 Plots showing the total radiative SERS Stokes cross-sections deduced from the measured differential cross-section using eqn (3) (red circles) and the pumping cross-sections (empty squares) for the spectra identified as being single molecule pumping events. The vibrational modes for which the cross-sections were measured are the (a) 802 cm^{-1}, (b) 914 cm^{-1} and (c) 1173 cm^{-1} of CV, as well as the (d) 593 cm^{-1} of NB. The different single molecule cases found in the maps are labeled with an arbitrary index (that simply counts them) along the horizontal axis. Note that the cross-sections are on a log-scale. Statistically speaking, there are a systematically larger values for the pumping (total) cross sections as compared to the Stokes (radiative) ones. The values for the pumping cross sections are obtained by assuming $A = 1$ and $\tau = 1$ ps. The possible effect of the asymmetry factor being $A \neq 1$ is discussed in the text.

V. Discussion

Of all the parameters that cannot be measured directly in these experiments, the vibrational lifetime τ is the least likely to have wide variations. A vibrational lifetime of ~ 100 ps, for example, cannot be forced into the analysis to justify an agreement between the Stokes and pumping determinations of the cross sections of specific cases. A τ of ~ 100 ps would imply an homogeneous broadening of the peak of ~ 0.3 cm^{-1} which is never seen in SM-SERS conditions.[23] One would be tempted at this stage to think that a vibrational lifetime of ~ 10 ps for all these modes would probably be enough to justify an agreement (of the average at least). A population lifetime of ~ 10 ps, however, would imply a contribution to the intrinsic linewidth of ~ 3 cm^{-1} and, therefore, would suggest that observed Raman peaks under SERS conditions have substantial contributions from *dephasing* to their intrinsic linewidths[24,25] (which is ~ 15–20 cm^{-1}). Inhomogeneous broadening of the peaks[24] has to be excluded, because the signals come from single molecules. Furthermore, even though a lifetime of 10 ps would explain the discrepancy for many of the events there are many others with pumping cross-sections that are 2 or 3 orders of magnitude larger than the Stokes cross-section which would require a lifetime of ~ 100–1000 ps which is completely unrealistic. Without a direct measurement of the lifetime by time resolved techniques under SERS conditions (never carried out to the very best of our knowledge) it is difficult to speculate further, but the possibility of everything being explained in terms of the lifetime seems far-fetched taking into account, in addition, that there are other possible contributions to the discrepancy, like the effect of the asymmetry factor and non-radiative effects which we now discuss.

A The asymmetry factor

The asymmetry factors of plasmon resonances—in clusters capable of producing SM-SERS—can be measured (with some difficulty) in a completely different type of experiment involving either dark-field illumination[26] or surface enhanced fluorescence[21] (only on the Stokes side of the spectrum). Itoh et al.,[26] for example, have carried out studies of typical surface plasmon resonances by dark field illumination in clusters similar to the ones used here, and correlating the extinction spectra of the resonances with the SERS signal itself. A correlation between the two was found, showing directly (experimentally) that the dispersion of the resonance is indeed the reason for asymmetries in the enhancement among different modes. The question is then reduced to the one of: how "steep" typical plasmon resonance can be in a window defined by a typical anti-Stokes-to-Stokes energy span. None of the observed resonances can really justify an asymmetry of two orders of magnitude between the anti-Stokes and Stokes peak, and this is particularly true for the peaks with the lowest Raman shifts (~ 500–600 cm^{-1}). The asymmetry must, in fact, disappear in the limit of zero Raman shift. In addition, if a considerable effect of asymmetries were present, there would also be a marked difference between modes at low and high Raman shifts in Fig. 4, and there is no experimental evidence for this at this stage. Other independent studies (performed by

This journal is © the Owner Societies 2009

Phys. Chem. Chem. Phys., 2009, **11**, 7372–7380 | 7377

ourselves, not shown here) on the correction of Raman intensities by the underlying SERS background in rhodamine 800 show basically the same conclusion: over a Raman-shift window of ~ 1000 cm^{-1} it is very difficult to observe resonances with dispersions that vary by more than a factor of ~ 2–5, with asymmetries of the order of ~ 10 found only in exceptional circumstances. Even though a factor of ~ 10 difference can—in some cases—marginally be ascribed to an asymmetry factor being responsible for the results (according to known asymmetry factors in typical plasmon resonances), many events can fluctuate by *two* orders of magnitude from this value, as shown in Fig. 4. It is these fluctuations by two orders of magnitude that cannot be easily ascribed to either variations in the asymmetry factors giving $A \neq 1$ for different single molecules at different places, or changes in the vibrational lifetime τ. If we only consider the pumping cross-section, it is possible to explain the fluctuation as being dominated by the asymmetry factor. However, explaining the discrepancy with the Stokes cross-section requires another mechanism which may be the non-radiative cross-section discussed in the next section.

B Non-radiative cross section

We would like to argue at this point that the statistically significant result of $\sigma^{\text{pump}} > \sigma_S^{\text{rad}}$ evidenced in Fig. 4 possibly suggests an additional effect contributing to the pumping cross section, to wit: the presence of non-radiative contributions to σ^{pump}. Admittedly, the possible contributions from non-radiative processes *cannot* be uniquely determined from these data, but it is (in our opinion) a distinct possibility which is not only expected on theoretical grounds[27] but also can help to bridge the gap in the experimentally observed difference between σ^{pump} and σ_S^{rad}, without having to stretch the values of either τ or A into seemingly unreasonable (and possibly unphysical) ranges. The possibility of non-radiative contributions to the pumping cross section deserves a brief detour into its origin.

The SERS cross section contains formally two main components: a radiative and a non-radiative one. This concept is further explained with the aid of Fig. 5. The reason for this is that SERS is *Raman scattering in (close) proximity to metals*, which possess their own optical properties and plasmon resonances[2] (and are therefore capable of absorbing light at different wavelengths). Under these conditions, there could be (for example) a photon reaching the molecule (the SERS probe) and producing a Stokes–Raman process (Fig. 5). However, the Stokes-shifted photon has a certain probability of being absorbed by the metal, thus never reaching the detector in the far-field. Formally, a Raman process *did* occur in the molecule, but we cannot detect it in the far-field. Accordingly, standard experiments measure the *differential radiative cross-section*, *i.e.* the number of photons that *do* make it to the detector (within the cone defined by the numerical aperture of the collecting optics). From it, an estimate of the total radiative cross-section σ_S^{rad} (Fig. 5(a)) can be obtained; *i.e.* the number of photons that would have been detected if our detector was covering all possible emission directions (for example using an integrating sphere). But there is a complementary number of Stokes–Raman processes that
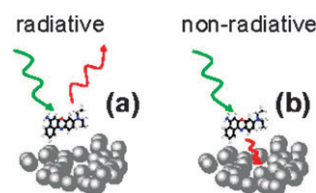

Fig. 5 Schematic representation of a *radiative* (a) and a *non-radiative* (b) SERS process. In (a), an incident photon (green) reaches the molecule and produces a Stokes-shifted Raman photon (red), which is scattered and detected in the far-field. In (b), on the contrary, the Stokes-shifted photon is absorbed by the metallic substrate and it is not detected in the far field. These latter events are not, therefore, detected as a SERS signal, but they *do* contribute to the vibrational population of the molecule through Stokes–Raman processes. This population is what is monitored subsequently on the anti-Stokes side with the technique of vibrational pumping. Accordingly, the vibrational population obtained from the Stokes signal (radiative cross section) underestimates the real population generated in the molecule which depends on both the radiative and non-radiative cross sections.

cannot detected since the corresponding photon is absorbed in the metal and not radiated, but they do occur and are represented by a *non-radiative cross-section* σ_S^{nrad} (Fig. 5(b)). The total SERS cross section (σ_S^{tot}) is the sum of the two:

$$\sigma_S^{\text{tot}} = \sigma_S^{\text{rad}} + \sigma_S^{\text{nrad}}. \tag{10}$$

It is possible to argue that the non-radiative cross section is mostly irrelevant, for it cannot be detected in the far-field as a Stokes process. But there is a notable exception to the rule in SERS that is particularly important for the experiments presented in this paper: the phenomenon of vibrational pumping. The latter is monitored as an anti-Stokes signal that depends on the vibrational population (achieved by Stokes processes) of the particular Raman active vibration being observed. The population, however, depends on *all* Stokes processes (radiative and non-radiative). Due to the presence of an "internal conversion process" inside the molecule (the generation of a vibrational population through Stokes scattering) we obtain a radiative signal (the anti-Stokes) that is proportional to the population and, therefore, to the *total* cross section. The estimation of cross sections with vibrational pumping using the anti-Stokes signal, therefore, will always tend to overestimate the *radiative* Stokes cross section, if the difference between total and radiative cross section is not introduced in the analysis. Within this framework, the pumping cross section σ^{pump} has to be identified with the *total* cross section for Stokes processes. This then adds an additional contribution to produce $\sigma^{\text{pump}} > \sigma_S^{\text{rad}}$.

In ref. 28 it was proposed that it may be possible to create a vibrational population through fluorescence processes in addition to the population created through Stokes scattering. The key difference between fluorescence pumping and Stokes pumping is that fluorescence pumping will create a vibrational population in all vibrational modes whilst Stokes pumping will only create a population in Raman active modes. It is therefore difficult to quantify how much fluorescence pumping contributes to the anti-Stokes intensity and hence we have ignored it in this study.

We summarize the main points of the experimental evidence presented here in the next section.

VI. Conclusions

The main conclusions of the evidence presented in our study, as well as some forward-looking observations, can be summarized as follows:

• The combination of the bi-analyte SERS method with low-temperature SERS vibrational pumping provides a rigorous demonstration of the possibility of observing single-molecule SERS vibrational pumping.

• The data in Fig. 4 has shown that there is a discrepancy between the pumping cross-section and the Stokes cross-section measured under single molecule conditions. The exact origin of this discrepancy is not obvious and several possibilities are explicitly considered in this paper. We believe that the source of the discrepancy can come from more than one origin, with two of the main effects being (i) the uncertainty in the parameters A and τ needed to infer σ^{pump}, and (ii) the presence of an additional physical mechanism contributing (and possibly dominating) the pumping cross-section, namely the non-radiative SERS processes.

• The span of cases in Fig. 4 is surely linked to the diversity of couplings experienced by different molecules with the metal surface, which could affect both its radiative and non-radiative cross-section independently. While the most likely reason for this is the diversity of asymmetry factors (A), it is also possible that different molecules will show different non-radiative cross sections.

• Above all, the results presented in this paper start closing a circle of a historical disagreement between claims of vibrational pumping cross sections and those determined solely from the Stokes signals. The fact that we are measuring on single molecules here avoids any possible complication with averaging over the enhancement distribution and it reveals that, indeed, the pumping cross sections is in general an overestimation of the "standard" radiative Stokes cross section. A distinction has to be made between *the experimental result*, which shows a clear and systematic difference between σ^{pump} and σ_S^{rad}, and the more speculative *interpretation of the experimental result* which suggest several possible origins for this difference (asymmetry factors, vibrational lifetimes, non-radiative components...).

• As far as SERS enhancement factors is concerned in these experiments, the integrated (not differential) non-SERS cross-section of CV is $\sim 10^{-25}$ cm^2,[7,29] which when taking the maximum Stokes cross-section at $\sim 10^{-16}$ cm^2 corresponds to an enhancement factor of $\sim 10^9$, which is in agreement with enhancement factors expected from theory,[3,14] and enhancement factors measured in the past.[7] Furthermore, we still see single molecule pumping events for Stokes cross-sections as low as $\sim 10^{-18}$cm^2, or an enhancement factor of $\sim 10^7$. These events are rare, however, and may be due to a favorable plasmon resonance. These values reinforce the idea that SERS enhancement factors that are $\sim 10^6$–10^7 times smaller than what originally deemed necessary ($\sim 10^{14}$) are enough to see single molecules, and that SM-SERS phenomena are a lot more common than what was originally suspected.[3]

In closing, we believe our paper presents the first consistent experimental evidence of SERS vibrational pumping in single molecules. Besides this being a definite step towards resolving several inconsistencies of past claims comparing different techniques, we hope that our results will pave the way to a deeper understanding of several subtle aspects of the SERS cross section (like non-radiative contributions) that will surely increase our ability to exploit the phenomenon and contribute to its furtherance.

References

1 R. Aroca, *Surface Enhanced Vibrational Spectroscopy*, Wiley, Chichester, 2006.
2 P. G. Etchegoin and E. C. Le Ru, in *Principles of Surface-Enhanced Raman Spectroscopy and Related Plasmonic Effects*, Elsevier, Amsterdam, 2009.
3 P. G. Etchegoin and E. C. Le Ru, *Phys. Chem. Chem. Phys.*, 2008, **10**, 6079.
4 M. Fleischmann, P. J. Hendra and A. J. McQuillan, *Chem. Phys. Lett.*, 1974, **26**, 163.
5 D. L. Jeanmaire and R. P. Van Duyne, *J. Electroanal. Chem.*, 1977, **84**, 1.
6 M. G. Albrecht and J. A. Creighton, *J. Am. Chem. Soc.*, 1977, **99**, 5215.
7 E. C. Le Ru, E. Blackie, M. Meyer and P. G. Etchegoin, *J. Phys. Chem. C*, 2007, **111**, 13794.
8 S. Shim, C. M. Stuart and R. A. Mathies, *ChemPhysChem*, 2008, **9**, 697.
9 K. Kneipp, Y. Wang, H. Kneipp, I. Itzkan, R. R. Dasari and M. S. Feld, *Phys. Rev. Lett.*, 1996, **76**, 2444.
10 R. C. Maher, P. G. Etchegoin, E. C. Le Ru and L. F. Cohen, *J. Phys. Chem. B*, 2006, **110**, 11757.
11 R. C. Maher, L. F. Cohen, E. C. Le Ru and P. G. Etchegoin, *J. Phys. Chem. B*, 2006, **110**, 19469.
12 R. C. Maher, C. M. Galloway, E. C. Le Ru, L. F. Cohen and P. G. Etchegoin, *Chem. Soc. Rev.*, 2008, **37**, 965.
13 H. W. Schroetter and H. W. Kloeckne, in *Raman Spectroscopy of Gases and Liquids*, ed. A. Weber, Springer, Berlin, 1979, p. 123.
14 E. C. Le Ru, P. G. Etchegoin and M. Meyer, *J. Chem. Phys.*, 2006, **125**, 204701.
15 E. C. Le Ru, M. Meyer and P. G. Etchegoin, *J. Phys. Chem. B*, 2006, **110**, 1944.
16 P. G. Etchegoin, M. Meyer, E. Blackie and E. C. Le Ru, *Anal. Chem.*, 2007, **79**, 8411.
17 E. Blackie, E. C. Le Ru, M. Meyer, M. Timmer, B. Burkett, P. Northcote and P. G. Etchegoin, *Phys. Chem. Chem. Phys.*, 2008, **10**, 4147.
18 P. C. Lee and D. Meisel, *J. Phys. Chem.*, 1982, **86**, 3391.
19 A. G. Brolo, A. C. Sanderson and A. P. Smith, *Phys. Rev. B: Condens. Matter Mater. Phys.*, 2004, **69**, 045424.
20 M. Meyer, E. C. Le Ru and P. G. Etchegoin, *J. Phys. Chem. B*, 2006, **110**, 6040.
21 E. C. Le Ru, P. G. Etchegoin, N. Félidj, J. Grand, G. Lévi and J. Aubard, *J. Phys. Chem. C*, 2007, **111**, 16076.
22 P. G. Etchegoin, E. C. Le Ru and M. Meyer, *J. Am. Chem. Soc.*, 2009, **130**, 181101.
23 J. A. Dieringer, R. B. Lettan II, K. A. Scheidt and R. P. Van Duyne, *J. Am. Chem. Soc.*, 2007, **129**, 16249.
24 W. Demtröder, *Laser Spectroscopy*, Springer, Berlin, 2003.
25 R. M. Shelby, C. B. Harris and P. A. Cornelius, *J. Chem. Phys.*, 1979, **70**, 34.

This journal is © the Owner Societies 2009

Phys. Chem. Chem. Phys., 2009, **11**, 7372–7380 | 7379

26 T. Itoh, K. Yoshida, V. Biju, Y. Kikkawa, M. Ishikawa and Y. Ozaki, *Phys. Rev. B:Condens. Matter Mater. Phys.*, 2007, **76**, 085405.
27 M. Moskovits, *Rev. Mod. Phys.*, 1985, **57**, 783.
28 H. X. Xu, X. H. Wang, M. P. Persson, H. Q. Xu, M. Kall and P. Johansson, *Phys. Rev. Lett.*, 2004, **93**, 243002.
29 Crystal Violet is one of the few molecules where the bare Raman cross sections can be obtained even in resonance conditions (see ref. 7). This is because the fluorescence of CV is quenched by non-radiative recombination processes and it therefore does not hide the resonant Raman signals of the modes (as it happens in more efficient emitters like NB with much higher quantum yields for the fluorescence).